Available online at www.sciencedirect.com
ScienceDirect
Geochimica et Cosmochimica Acta 75 (2011) 4295–4309
Geochimica et Cosmochimica Acta
www.elsevier.com/locate/gca

Changes in water extractable organic matter during incubation of forest floor material in the presence of quartz, goethite and gibbsite surfaces

Katherine Heckman [a,*], Angelica Vazquez-Ortega [b,1], Xiaodong Gao [b,1], Jon Chorover [b,1], Craig Rasmussen [b,1]

[a] USDA Forest Service, Center for AMS, L-397, 7000 East Ave., Livermore, CA 94550, USA
[b] Dept. of Soil, Water and Environmental Science, University of Arizona, P.O. Box 210038, Tucson, AZ 85721-0038, USA

Received 11 January 2011; accepted in revised form 9 May 2011; available online 18 May 2011

Abstract

The release of dissolved organic matter (DOM) from forest floor material constitutes a significant flux of C to the mineral soil in temperate forest ecosystems, with estimates on the order of 120–500 kg C ha^{-1} $year^{-1}$. Interaction of DOM with minerals and metals results in sorptive fractionation and stabilization of OM within the soil profile. Iron and aluminum oxides, in particular, have a significant effect on the quantity and quality of DOM transported through forest soils due to their high surface area and the toxic effects of dissolved aluminum on microbial communities. We directly examined these interactions by incubating forest floor material, including native microbiota, for 154 days in the presence of (1) goethite (α-FeOOH), (2) gibbsite (γ-$Al(OH)_3$), and (3) quartz (α-SiO_2) sand (as a control). Changes in molecular and thermal properties of water extractable organic matter (WEOM, as a proxy for DOM) were evaluated. WEOM was harvested on days 5, 10, 20, 30, 60, 90, and 154, and examined by thermogravimetry/differential thermal analysis (TG/DTA) and diffuse reflectance Fourier transform infrared (DRIFT) spectroscopy. Results indicated significant differences in WEOM quality among treatments, though the way in which oxide surfaces influenced WEOM properties did not seem to change significantly with increasing incubation time. Dissolved organic C concentrations were significantly lower in WEOM from the oxide treatments in comparison to the control treatment. Incubation with goethite produced WEOM with mid-to-high-range thermal lability that was depleted in both protein and fatty acids relative to the control. The average enthalpy of WEOM from the goethite treatment was significantly higher than either the gibbsite or control treatment, suggesting that interaction with goethite surfaces increases the energy content of WEOM. Incubation with gibbsite produced WEOM rich in thermally recalcitrant and carboxyl-rich compounds in comparison to the control treatment. These data indicate that interaction of WEOM with oxide surfaces significantly influences the composition of WEOM and that oxides play an important role in determining the biogeochemistry of forest soil DOM.
Published by Elsevier Ltd.

1. INTRODUCTION

The importance of soil organic C to the global C cycle is well-recognized (e.g., Amundson, 2001). Yet despite decades of research, many questions remain as to how physical, chemical and biological soil processes interact to control soil organic C stabilization (cf. von Lützow et al., 2006). In this context, the present study focuses specifically on the biogeochemistry of dissolved soil organic matter (DOM) and how biodegradation of organic materials in the presence of oxide surfaces alters DOM chemical and physical properties. While DOM comprises only ~1% of the total soil organic carbon pool, it is the most mobile

* Corresponding author. Tel.: +1 925 422 9556; fax: +1 925 423 7884.
E-mail address: kaheckman@fs.fed.us (K. Heckman).
[1] Tel.: +1 520 621 1646; fax: +1 520 621 1647.

0016-7037/$ - see front matter Published by Elsevier Ltd.
doi:10.1016/j.gca.2011.05.009

fraction (Zsolnay, 1996), and is thought to be the largest source of new C inputs to subsurface soils in temperate forest systems (Zech and Guggenberger, 1996; Kaiser and Guggenberger, 2000; Michalzik et al., 2001; Rumpel and Kögel-Knabner, 2010).

A number of chemical, physical and biological processes control DOM degradation rates in soil environments. In the initial stages of biodegradation, or in the absence of mineral materials, the relative structural recalcitrance of organic matter may play a dominant role in determining the mean residence time (Kalbitz et al., 2003a,b; Nierop et al., 2003). However, long-term persistence of organic matter in soils is generally attributed to protective complexation mechanisms such as binding to oxides and secondary phyllosilicates, as well as interaction with polyvalent metal cations (Al^{3+}, Fe^{3+}) to form organo-metal complexes (Mikutta et al., 2006; Marschner et al., 2008). Such physicochemical interactions with mineral surfaces have long been recognized as key factors controlling soil organic matter content (Greenland, 1971; Martin and Haider, 1986; Theng and Tate, 1989; Baldock and Skjemstad, 2000). Sorption of soil organic matter to mineral surfaces has additional important effects on the soil system, including changes in the surface properties of minerals and potential influence on microbial community composition and function (Heckman et al., 2009).

Goethite and gibbsite are ubiquitous in soils (Kampf et al., 2000) and have a significant impact on organic C cycling due to their high specific surface area and abundance of reactive hydroxyl groups. As DOM moves through the soil profile, Fe and Al oxides interact with organics in solution through surface sorption as well as the formation of organo-metal complexes from Fe and Al cations released during mineral dissolution (Kaiser and Zech, 2000; Kaiser and Guggenberger, 2000). Hydroxyl and carboxyl functional groups of dissolved organics can form strong inner-sphere complexes with goethite and gibbsite surfaces through ligand exchange reactions (Parfitt et al., 1977; Gu et al., 1994; Molis et al., 2000; Chorover and Amistadi, 2001), or can be more weakly sorbed through hydrophobic interactions, electrostatic interactions and hydrogen bonding (Evanko and Dzombak, 1999; Stevenson, 1994). Formation of organo-metal complexes involves bonding of reactive organic functional groups with dissolved metal ions, which induces chemical and conformational changes in the organics and reduces their susceptibility to enzyme attack (Byler et al., 1987; Baldock and Skjemstad, 2000; Nierop et al, 2002; Scheel et al., 2007). Such interactions have been hypothesized to decrease the biodegradability of DOM, and increase C mean residence times by slowing the decomposition process (Boudot et al., 1989; Veldkamp, 1994; Torn et al., 1997; Jones and Edwards, 1998; Eusterhues et al., 2003; Masiello et al., 2004). However, how the influence of oxide surfaces on DOM characteristics may change during active biodegradation of natural organic materials is not well constrained.

Sorption of organics to hydrous oxide surfaces has been well studied under controlled abiotic laboratory conditions. Previous experiments using leaching columns and batch isotherm experiments have demonstrated preferential sorption of specific classes of organics to Fe- and Al-oxyhydroxides. These organics include high molecular weight compounds, compounds rich in N or P, compounds with reactive acidic groups, and aromatic compounds (McKnight et al., 1992; Stevenson, 1994; Gu et al., 1994; Meier et al., 1999; Stevenson and Cole, 1999; Chorover and Amistadi, 2001; Zhou et al., 2001). Though such batch and column studies have allowed us to identify characteristics and bonding mechanisms that affect short-term abiotic DOM fractionation and preferential adsorption, they have not captured the longer-term dynamics of mineral-DOM interactions in biologically active media with ongoing biodegradation and variable microbial communities.

To address this knowledge gap, we conducted long-term (>150 day) incubations of forest floor material inoculated with their native microbial community in the presence of quartz, goethite and gibbsite surfaces. Water extractable organic matter (WEOM) was used as a proxy for dissolved organic matter. These experiments yielded the unique opportunity to track the co-evolution of WEOM properties and microbial community dynamics throughout the biodegradation process. Here we present details on the control of WEOM physical and chemical characteristics by goethite and gibbsite surfaces. We employed DRIFT, TG/DTA, and other basic quantitative measures of WEOM quality such as pH, molar absorptivity, and concentrations of Fe and Al in WEOM solutions to quantify these effects.

2. METHODS

2.1. Characterization of minerals

Minerals used in the incubation experiment were thoroughly characterized prior to use. Quartz sand was purchased from Fisher Scientific (Pittsburgh, PA). Prior to incubation, the sand was submerged in 30% H_2O_2 (1:1 weight to volume ratio) and shaken for 24 h to remove any pre-existing organic matter contamination. Sand was rinsed three times with deionized water, then submerged in 1 M HCl (1:1 weight to volume ratio) and shaken for 24 h to remove any exchangeable cations. The sand was then rinsed with deionized water until the pH and EC of the rinse water matched that of the deionized water. The sand was then dried at 110 °C and stored in an acid-washed sterile container until use.

Goethite and gibbsite were purchased from Ward's Natural Science (Rochester, NY). Phase purity was confirmed by X-ray diffraction. Minerals were analyzed as random powder mounts from 2 to 70° 2θ on a PANalytical X'Pert PRO-MPD X-ray diffraction system (PANalytical, Almelo, AA, The Netherlands) producing Cu-Kα radiation at an accelerating potential of 45 kV and current of 40 mA, and fitted with a graphite monochromator and sealed Xenon detector. Particle size was measured on a Beckman Coulter LS 13 320 Laser Diffraction Particle Size Analyzer (Beckman Coulter Inc., Fullerton, CA). Specific surface area was determined via N_2 adsorption on a Beckman Coulter SA 3100 Gas Adsorption Surface Area Analyzer (Beckman Coulter Inc., Fullerton, CA), and calculated according to the BET theory (Brunauer et al., 1938). Particle size and

specific surface area measurements were made on three subsamples of each mineral type.

All mineral samples were well homogenized prior to examination. There was no noticeable variation among mineral subsamples for any of the parameters measured (standard error of experimental replicates was at or close to zero). All minerals were pure phases as determined by X-ray diffraction. Particle size and specific surface area varied among the minerals. Quartz, goethite, and gibbsite particles had a mean diameter of 211, 23, and 14 μm and specific surface area of 0.03, 3.51, and 1.32 $m^2\ g^{-1}$, respectively.

2.2. Experimental design

Natural forest floor organic material was incubated after inoculation with a natural forest floor microbial community in three mineral matrices: quartz sand mixed with goethite; quartz sand mixed with gibbsite; and quartz sand alone (as a control treatment). The matrices for each treatment were as follows: (i) Control treatment: 30 g quartz sand; (ii) Goethite treatment: 6 g goethite grains and 24 g quartz sand; and (iii) Gibbsite treatment: 6 g gibbsite grains and 24 g quartz sand. Quartz sands were included in the goethite and gibbsite treatments to reduce the oxide content of the mineral matrices to ratios more approximately resembling the oxide abundance in natural soils as well as to ensure adequate porosity in the oxide treatments.

Organic material used in the incubation experiment consisted of partially decomposed material collected from the full forest floor (Oi, Oe, Oa horizons) in an Arizona forest dominated by *Pinus ponderosa* in the overstory (see Heckman et al., 2009 for site details). Forest floor material was dried at 30 °C, cut to pieces measuring ~1 cm in length and homogenized using a blender. Total C, N and $\delta^{13}C$ of the forest floor material was determined by high temperature dry combustion with an elemental analyzer (Costech Analytical Technologies, Valencia, CA, USA) coupled to a continuous-flow mass spectrometer (Finnigan Delta Plus-XL, San Jose, CA, USA) at the University of Arizona Stable Isotope Laboratory. The homogenized forest floor material was 43%C and 1%N by weight with a $\delta^{13}C$ value of −26‰. Three grams of homogenized forest floor material were mixed with the respective quartz sand, gibbsite or goethite treatments in 125 ml glass jars (Fisherbrand, Fisher Scientific).

Microbial inoculum derived from field collected organic horizon material was prepared following Wagai and Sollins (2002). Freshly collected forest floor material was mixed with deionized water at a mass to volume ratio of 1:5. The mixture was shaken vigorously for 30-min on a reciprocal shaker followed by overnight shaking on a low frequency setting. After 12 h of slow shaking, the mixture was vacuum filtered through a 5-μm polycarbonate membrane filter. Vacuum line pressure was kept below 69 kPa (equivalent to 51.7 cm Hg or 20.4 in Hg) to prevent lysing of microbial cells. Filtrate was stored in a sterilized bottle overnight at 4 °C before use. A 1 ml aliquot of inoculum solution was added to each jar.

Samples were homogenized, wetted to 60% of water holding capacity (Cassel and Nielsen, 1986) with deionized water, and tamped to a uniform bulk density. Sample cups were placed in 950 cm^3 mason jars. Soil moisture was maintained by the addition of 3 ml of water to the bottom of each jar to maintain 100% relative humidity within the jar atmosphere. Aerobic conditions in the sample jars were maintained by opening the jars and venting the samples periodically. Headspace CO_2 concentrations were monitored and were not permitted to exceed 3% by volume at any time during the incubation. Samples were incubated at 25 °C, and analyzed at seven time intervals: 5, 10, 20, 30, 60, 90 and 154 d. Each time interval was replicated in triplicate for each mineral treatment for a total of 63 samples. All 63 samples were prepared simultaneously and incubations were initiated at the same time. At the end of each time interval, three replicates from each treatment were destructively sampled. Samples were mixed with a spatula, and 12 g of homogenized material were removed and frozen to be used for microbial analysis at a later time. The remainder of the sample was mixed with deionized water in a 15:1 solution to solid mass ratio and shaken on a side-to-side shaker for 24 h. Samples were vacuum filtered, first through a 1 μm glass fiber A/E filter, then through a 0.22μm polymer filter (Millipore type GV). The filtrate was considered to contain the WEOM fraction and was stored in sterilized bottles at 4 °C until elemental, molecular mass, and UV–Vis spectrometry analyses were completed. The WEOM was then lyophilized prior to performing DRIFT and TG/DTA analyses.

Incubation conditions were not intended to precisely reproduce the full complexity of a natural soil environment. Rather, our intent was to employ a controlled model system in order to reduce the number of factors influencing WEOM qualities. Gibbsite and goethite grain size was somewhat larger than that which may be found in soils (silt sized as opposed to clay sized), with the effect that the amount of exposed oxide surface area may be lower in the incubation than would be expected in a natural soil. The incubation conditions provide optimum temperature and moisture for microbial growth. Incubation of soils and substrates under controlled laboratory conditions is a widely accepted method (Zibilske, 1994) that enables well-constrained comparison of respiration rates and WEOM properties among mineral treatments (e.g., Mikutta et al., 2007).

2.3. Water extractable organic matter analysis

2.3.1. C, N, Fe, Al concentrations and molecular mass

Total organic C (non-purgeable) and total N of the WEOM solutions were measured on a Shimadzu TOC-VCSH analyzer (Columbia, MD). Solution Fe and Al concentrations were determined by inductively coupled plasma mass spectrometry (ICP-MS) on a Perkin–Elmer Elan DRC II ICP-MS (Waltham, MA). Concentrations of C, N, Fe, and Al were expressed relative to grams of litter C, with all values normalized to the C content of the solid phase sample prior to incubation [$g\ C\ g^{-1}$ litter C]. Apparent weight averaged molecular mass (MW_{APP}) of the WEOM solutions was measured by size exclusion high performance liquid chromatography on a Waters High Performance

Liquid Chromatography System (Agilent Technologies, Palo Alto, CA). Solutions were diluted to a concentration of 50 mM of C L^{-1} in a sodium phosphate solution buffered to pH 5.5. WEOM solutions from unincubated forest floor material were also analyzed for comparison with the incubation treatments.

2.3.2. Ultraviolet–visible spectroscopy

Ultraviolet–visible spectra were obtained with a Shimadzu UV-Probe PC2501 UV–Vis spectrophotometer (Columbia, MD). Absorbances were recorded at 254, 280 and 365 nm. Prior to measurement, samples were diluted with sodium phosphate buffer (pH 5.5) both to standardize solution pH values among the treatment groups and ensure that all absorbance values were <0.7. Absorbances at 280 nm were divided by the molar concentration of dissolved organic C in WEOM extracts to give "molar absorptivity" or specific UV absorbance (SUVA). Molar absorptivity at 280 nm is commonly accepted as an index of WEOM aromaticity (Chin et al., 1994; Peuravuori and Pihlaja, 1997). The quotient of absorbance at 254 nm to that at 365 nm (E_2:E_3) is correlated with absorption from specific chromophores containing unbonded electrons and has been related to the molecular size of WEOM (Peuravuori and Pihlaja, 1997; Guo and Chorover, 2003). Low E_2:E_3 values are generally associated with higher molar mass constituents.

2.3.3. Infrared spectroscopy

WEOM was lyophilized after all other analyses were completed. The freeze-dried WEOM was mixed with KBr in a 1:20 w/w ratio (WEOM:KBr). Diffuse reflectance infrared Fourier transform (DRIFT) spectra were recorded using a Nicolet 560 Magna IR Spectrometer (Madison, WI). Samples were mixed with KBr, pressed gently into metal cups, and scanned over the 4000–400 cm^{-1} range. Four hundred scans were averaged for each spectrum at a resolution of 4 cm^{-1} and normalized by using pressed pure KBr as background. An automatic baseline correction was applied to each spectrum to remove baseline distortions. Spectral analysis, including peak deconvolution and integration, was performed using the GRAMS/AI Spectroscopy Software Suite (Thermo Scientific).

2.3.4. Thermal analysis

Thermogravimetric (TG) and differential thermal analyses (DTA) were conducted on lyophilized WEOM samples using a Diamond series TG/DTA (Perkin–Elmer; Shelton, CT). A four point calibration using indium, tin, zinc, and silver standards was used to determine the conversion factor from electrical potential ($\mu V\ s^{-1}$) to heat flow (mW). TG and DTA data were recorded simultaneously. The reference pan contained calcinated α-Al_2O_3 powder. Due to the limited sample size, WEOM samples that were diluted with KBr for DRIFT analysis were also used for TG-DTA analysis (1:20 dilution ratio, WEOM:KBr). KBr is thermally inert from room temperature to 734 °C. To confirm that the presence of KBr would not cause artifacts in the data, several samples of WEOM were measured after dilution with both KBr and alumina. No differences were detected between the KBr and alumina profiles, therefore KBr was assumed to have no effect on the thermal data. Sample mixtures were heated from 50 to 650 °C, at a rate of 20 °C min^{-1} with continuous air flow of 50 ml min^{-1}. DTA peak integration was conducted using Origin 7.5 (OriginLab Corporation; MA). DTA profiles of mW versus time were integrated, yielding units of kJ per peak or per profile (total enthalpy of combustion). Enthalpy values (in kJ) were then divided by mass loss or total sample mass to give values of kJ $g_{mass\ loss}^{-1}$ or kJ g_{mass}^{-1}. Total sample mass refers to the mass of lyophilized WEOM only, and excludes the mass of KBr.

2.4. Statistical methods

Each sample harvested at a specific destructive sampling period was treated as a replicate for a given treatment, providing three replicates for each treatment per sample time and a total of 21 replicates per treatment across all time periods. Significant differences between WEOM properties among treatments were determined by two-way ANOVA using mineral treatment (goethite, gibbsite or control/quartz) and time as the main effects followed by Tukey–Kramer *post hoc* test at a 95% confidence limit ($n = 21$ for each mineral treatment). Significant differences among DRIFT and TG/DTA peak areas were determined by one-way ANOVA by mineral type followed by Tukey–Kramer *post hoc* test at a 95% confidence limit. Only one spectrum (for both DRIFT & TG/DTA) per treatment per time period was analyzed for peak areas ($n = 7$ for each mineral treatment). Linear regression was used to assess trends in DRIFT and TG/DTA peak areas over time and to investigate correlations among measured WEOM properties.

3. RESULTS

3.1. Carbon and nitrogen

Dissolved organic carbon (DOC) concentrations were significantly lower in oxide treatments relative to the control when averaged over time with values of control = 20.3, goethite = 10.0, and gibbsite = 9.6 mg g^{-1} litter C (Table 1). These differences were mostly due to two large spikes in DOC concentration at 20 and 60 days in the control treatment. In comparison, DOC concentrations of the oxide treatments did not exhibit large fluctuations as seen in the control treatment (Table 1). By day 154, there was no statistical difference in DOC concentration between the control and oxide treatments, and DOC concentrations in all treatments had decreased by approximately 60% over the course of the incubation.

C:N ratios were not significantly different among treatments and all treatments exhibited variation over time (Table 1). However, C:N ratios did decrease from day 60 to day 154, and C:N ratios were an order of magnitude lower at the end of the incubation than at the beginning, i.e., C:N of ~100 at day 5 versus ~21 at day 154.

For comparison, C and N content of WEOM solutions from unincubated forest floor material were also measured. Values for these solutions are listed in Table 1 under the treatment label "Forest Floor".

Table 1
Characteristics of water extractable organic matter solutions.

Treatment	Incubation length days	DOC [a] mg $g_{litter\ C}^{-1}$	C:N	pH	Fe:C $mmol_{Fe}:mol_{DOC}$	Al:C $mmol_{Al}:mol_{DOC}$	Mw_{AP} Daltons	E_2/E_3	Molar absorptivity A mol_C^{-1}
Forest floor	0	9.8 (0.2)	39 (2)	5.38 (0.02)	–	–	3468 (40)	5.8 (0.3)	207.6 (2.3)
Control	5	17.8 (3.5)	119.5 (23.9)	5.62 (0.03)	0.09 (0.03)	0.91 (0.23)	2957 (42)	5.7 (0.2)	44.6 (8.8)
	10	13.0 (1.7)	66.1 (14.2)	5.00 (0.07)	0.14 (0.02)	0.74 (0.11)	4951 (1815)	5.4 (0.1)	52.1 (8.7)
	20	41.1 (12.2)	221.7 (80.1)	5.75 (0.01)	0.06 (0.01)	0.26 (0.06)	2760 (194)	6.9 (0.1)	15.4 (3.6)
	30	8.1 (2.5)	42.5 (18.4)	5.62 (0.02)	0.32 (0.08)	1.26 (0.33)	4218 (681)	5.5 (0.1)	87.1 (22.8)
	60	46.7 (6.0)	88.1 (7.6)	6.06 (0.03)	0.06 (0.01)	0.27 (0.03)	2951 (12)	6.1 (0.1)	88.1 (1.4)
	90	10.1 (0.9)	61.4 (11.7)	6.13 (0.04)	0.21 (0.01)	0.86 (0.10)	2723 (27)	5.9 (0.1)	63.7 (5.3)
	154	5.8 (0.2)	27.3 (13.2)	6.25 (0.02)	0.44 (0.07)	2.47 (0.05)	3904 (30)	7.1 (0.6)	102.5 (0.9)
	Average over time	20.3^{A}	89.5^{A}	5.78^{B}	0.19^{B}	0.97^{B}	3495^{A}	6.1^{A}	64.8^{A}
Goethite	5	15.2 (2.7)	128.4 (29.7)	5.95 (0.07)	2.91 (0.7)	0.56 (0.32)	1604 (105)	2.8 (0.2)	32.4 (4.4)
	10	9.6 (1.6)	60.2 (12.9)	5.71 (0.17)	5.91 (1.17)	0.25 (0.07)	1600 (123)	3.3 (0.1)	39.8 (5.9)
	20	14.4 (1.5)	32.0 (8.5)	5.41 (0.27)	7.05 (1.7)	0.22 (0.07)	1702 (295)	3.3 (0.7)	26.5 (1.8)
	30	11.3 (3.3)	80.5 (25.1)	5.92 (0.01)	8.74 (1.61)	0.03 (0)	2024 (292)	2.6 (0.2)	29.5 (12.6)
	60	7.2 (2.3)	219.5 (0.00)	6.10 (0.01)	16.00 (3.98)	0.5 (0.12)	2371 (8)	2.5 (0.1)	77.3 (18.3)
	90	8.3 (1.5)	57.1 (1.0)	6.27 (0.04)	2.98 (0.75)	0.37 (0.08)	2071 (95)	3.1 (0.2)	47.7 (10.6)
	154	4.1 (0.4)	19.0 (2.0)	6.35 (0.02)	32.75 (6.04)	1.62 (0.24)	3016 (224)	2.6 (0.1)	114.3 (17.4)
	Average over time	10.00^{B}	85.2^{A}	5.96^{AB}	10.91^{A}	0.51^{B}	2056^{B}	2.9^{B}	52.5^{A}
Gibbsite	5	11.5 (1.7)	65.5 (21.5)	6.17 (0.02)	0.2 (0.03)	3.72 (0.43)	1763 (27)	5.6 (0.3)	46.5 (6.1)
	10	10.5 (1.8)	80.2 (20.7)	5.92 (0.01)	0.08 (0.01)	1.78 (0.17)	2144 (27)	5.6 (0.0)	44.5 (4.7)
	20	16.9 (7.2)	54.5 (52.1)	5.20 (0.57)	0.27 (0.18)	2.81 (0.98)	2043 (204)	7.6 (0.1)	34.0 (10.7)
	30	7.0 (1.1)	47.6 (4.1)	5.95 (0.01)	0.68 (0.47)	3.2 (0.11)	2152 (79)	5.6 (0.0)	57.4 (5.7)
	60	11.7 (1.8)	83.9 (0.8)	6.15 (0.01)	0.14 (0.02)	3.16 (0.45)	2800 (22)	6.1 (0.1)	40.2 (5.7)
	90	5.5 (0.5)	42.1 (3.5)	6.40 (0.01)	0.28 (0.01)	6.14 (0.13)	2840 (492)	5.9 (0.0)	78.8 (3.9)
	154	4.2 (0.1)	16.1 (12.0)	6.52 (0.04)	3.40 (0.02)	8.88 (0.35)	4835 (318)	7.0 (0.8)	83.6 (2.4)
	Average over time	9.6^{B}	55.7^{A}	6.05^{A}	0.28^{B}	4.24^{A}	2654^{B}	6.2^{A}	55.0^{A}

[a] Specifically: dissolved organic carbon, measured as milligrams of C in the dissolved organic C fraction, divided by the total grams of C in the solid sample prior to incubation Values at each time point are the average of three replicates for each treatment ($n = 3$). "Average over time" values are the average of all replicates across time ($n = 21$). Significance was determined using two-way ANOVA with treatment and time as main effects, followed by Tukey's HSD *post hoc* test ($a = 0.05$). Within each column, means followed by different superscript letters are significantly different.

3.2. pH and metal: C ratios

The pH of WEOM solutions extracted from the forest floor material prior to exposure to oxide surfaces or incubation was 5.4 (see Table 1, "Forest Floor" values). The pH values of all treatments exhibited large fluctuations early in the incubation, then steadily increased from day 30 to day 154 (Table 1). When averaged across time, the pH values of the WEOM solutions were higher for the oxide treatments than for the controls, with gibbsite = 6.05, goethite = 5.96, and control = 5.78. The pH of WEOM solutions from the gibbsite treatment were significantly greater than those of the controls (Table 1). The change in pH was particularly interesting given that pH exerts strong control on the formation of metal-humus complexes. Solution pH strongly influences both the solubility of Fe- and Al-oxides and organic matter, and affects the type of bonding favored between metals and organics, the rate and abundance of organo-metal complex formation, and the speciation of dissolved metals (Lindsay, 1997; Plankey and Patterson, 1987; Gu et al., 1994; Stevenson, 1994; Guan et al., 2006).

Aqueous metal:C ratios were relatively low throughout the incubation, but increased over time (Table 1). Among oxide treatments, Fe:C reached a maximum of 33 mmol Fe per mol C at day 154 of the incubation in the goethite treatment, whereas Al:C reached a maximum of 9 mmol Al per mol of C at day 154 of the incubation in the gibbsite treatment. Low metal:C ratios were most likely due to the low solubility of both goethite and gibbsite at circum neutral pH values. The stability of gibbsite is at its maximum at pH values ~7.5, and is still quite stable at a pH of 6.0 to 6.5 (Lindsay, 1997). Goethite is most stable at pH values of ~8, but still has low solubility at pH of 6.0–6.5 (Cornell and Schwertmann, 1996).

While absolute metal concentrations were relatively low over the course of the incubation, they were several orders of magnitude higher than those predicted from mineral solubility constants for inorganic, monomeric Al and Fe alone. Concentrations of Al in WEOM from the gibbsite treatment were on the order of 10^{-5} to 10^{-6} mol L^{-1}, whereas inorganic Al in equilibrium with gibbsite at this pH is on the order of 10^{-10} mol L^{-1}. Solution Fe concentrations in WEOM from the goethite treatment were 10^{-4} to 10^{-5} mol L^{-1}, whereas equilibrium of inorganic Fe with goethite gives Fe concentrations on the order of 10^{-18} mol L^{-1} (Lindsay, 1997).

Evidently, goethite exhibited greater dissolution than gibbsite during the incubation. The differences in apparent solubility may be controlled in part by a kinetic effect induced by variation in mineral specific surface area; specific surface area of goethite was nearly three times that of gibbsite (3.51 and 1.32 $m^2 g^{-1}$ for goethite and gibbsite, respectively). The XRD data also indicated gibbsite exhibited greater crystallinity than goethite, which may also contribute to lower solubility (Schwertmann, 1991). If metal-DOM complexes are substantially more stable for Fe than for Al, this would also contribute to a higher total concentration of Fe than Al in solution. Finally, it is possible that reductive dissolution of Fe (III) may have occurred in localized anoxic areas of the incubating substrate, resulting in relatively higher aqueous Fe concentration (Schwertmann, 1991).

3.3. Apparent molar mass of WEOM

The apparent molar mass of WEOM from the control treatment exhibited moderate fluctuation over time, whereas that of WEOM from the goethite and gibbsite treatments steadily increased over the course of the incubation (Table 1). The apparent molar mass of WEOM from all treatments increased significantly over time (time versus Mw_{APP}: $r^2 = 0.20$, $p = 0.044$). When averaged across time, WEOM from the control treatment had a significantly higher apparent molar mass than WEOM from both the goethite and gibbsite treatments ($p = 0.0022$).

Mw_{APP} and metal:C were significantly and positively correlated in both the goethite ($r^2 = 0.84$, $p = 0.0035$) and gibbsite ($r^2 = 0.76$, $p = 0.0107$) treatments, but not in the control treatment ($r^2 = 0.16$, $p = 0.3792$). These correlations suggest that the Mw_{APP} values were affected by the presence of dissolved metals and the formation of metal-humus complexes, and may not reflect the Mw of uncomplexed WEOM components deriving from the goethite and gibbsite treatments.

3.4. Ultraviolet–visible spectroscopy

E_2:E_3 ratios of gibbsite and control treatments were nearly equivalent with average E_2:E_3 of 6.1 and 6.2 for control and gibbsite, respectively throughout the incubation. The ratio increased slightly from day 5 to day 154 by approximately 1 unit in both treatments. The E_2:E_3 values of the goethite treatment were significantly lower ($p < 0.0001$) than gibbsite and control values and did not vary or increase over time; average E_2:E_3 of goethite WEOM was 2.9. The E_2:E_3 can provide a proxy of molar mass with low E_2:E_3 values generally associated with high molecular weights (Peuravuori and Pihlaja, 1997; Guo and Chorover, 2003). In the current study, however, E_2:E_3 was poorly correlated with apparent molecular weight ($r^2 = 0.23$ for Mw_{APP} versus E_2:E_3), likely because of the effect of metal complexation on increasing apparent molar mass, as discussed above (see Section 3.3).

Molar absorptivity exhibited large fluctuations over time in all treatments (Table 1), but did increase significantly over time in all treatments (time versus molar absorptivity: $r^2 = 0.58$, $p < 0.0001$). Molar absorptivity was not significantly different among treatments.

3.5. DRIFT spectroscopy

All treatments yielded similar DRIFT spectra for WEOM samples but with consistent, treatment dependent variation in relative peak areas (Fig. 1). The spectra from the gibbsite incubations exhibited peaks from 3450 to 3650 cm^{-1} attributable to metal-OH stretching that were absent in the control and goethite treatment spectra. All other major peaks were present in all three treatments. Peaks were assigned as indicated in Table 2.

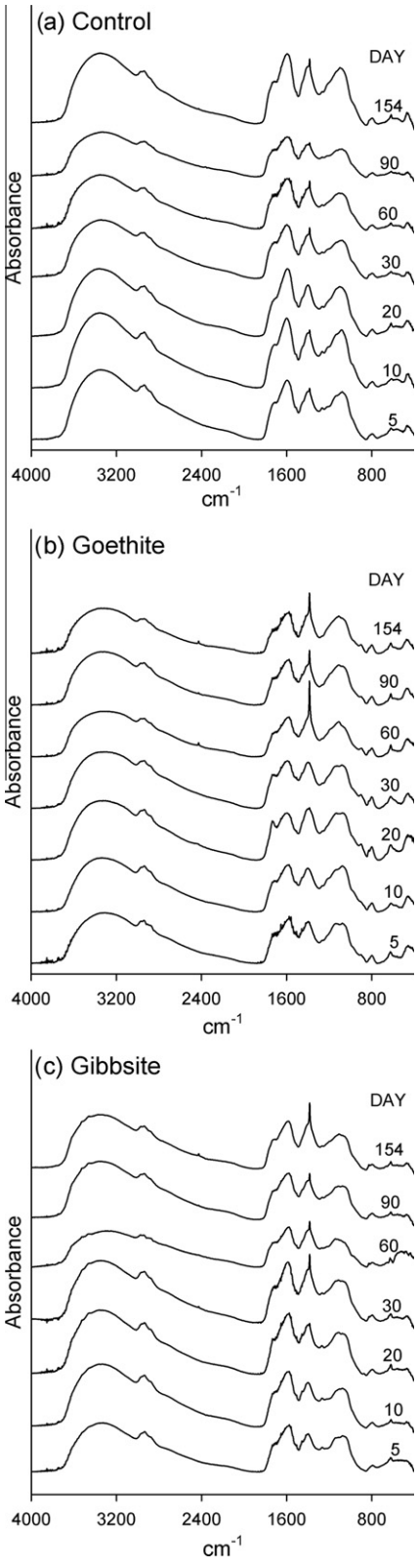

Fig. 1. DRIFT spectra for WEOM from each treatment at each sampling time during the incubation. (a) Control treatment: quartz sand and forest floor material, (b) Goethite treatment: quartz sand mixed with goethite and forest floor material, (c) Gibbsite: quartz sand mixed with gibbsite and forest floor material.

Deconvolution of DRIFT spectra revealed differences in the structural characteristics of WEOM among treatments (Table 3). Peak areas of the three treatments were calculated for six major bond types/regions: Amide I band (1650 cm^{-1}), polysaccharides (calculated as the sum of peaks at 1240, 1140, 1055, 950 and 900 cm^{-1}), metal + COO^- bonds (1380 cm^{-1}), esters (1730 cm^{-1}), $\nu_{as}COO^-$ (asymmetric carboxyl peak at 1580 cm^{-1}), and ν metal-OH (metal-OH stretches at 3500 and 3530 cm^{-1}). In general, WEOM from the goethite treatment was significantly different from the control in many respects, whereas WEOM from the gibbsite treatment was rarely significantly different from either the control or the goethite treatment.

Amide I band areas were significantly lower in WEOM from the goethite treatment than from the other treatments, indicating lower protein content in WEOM from the goethite treatment. Assuming equivalent WEOM production, the lower protein content indicates a preferential adsorption of proteins to goethite surfaces, consistent with previous research (Omoike and Chorover, 2006). Similarly, the ratio of the amide I band area to the sum of the polysaccharide peak areas (Amide I:Σ Polysaccharide) was significantly higher in the controls than in the goethite treatment (control^a > gibbsite^{ab} > goethite^b), also suggesting goethite surface preference for proteinaceous compounds. The area of the ester peak, (~1730 cm^{-1}) commonly associated with fatty acids, was also significantly higher in the control treatment than in the goethite treatment (control^a > gibbsite^{ab} > goethite^b) suggesting preferential adsorption of fatty acids to the goethite surfaces. The "νCOO-metal" peak areas were significantly different among treatments (goethite^a > gibbsite^{ab} > control^b), indicating a greater abundance of carboxyl-metal bonds formed in the goethite treatment.

Peak deconvolution allowed separation of the amide I band from the asymmetric carboxyl peak, revealing a peak centered at ~1380 cm^{-1} in all spectra. This peak exhibited distortion in the form of narrowing and "pointiness" in some spectra, particularly in those spectra for longer incubation times. This peak is due to symmetric $-COO^-$ stretching, and the distortion or narrowing is related to carboxylate-metal bond formation (Fu and Quan, 2006; Gu et al., 1994). The observed peak distortion is consistent with the measured concentrations of Al and Fe in excess of mineral solubility observed in corresponding solutions; higher concentrations of dissolved Al and Fe are associated with greater distortion of the 1380 cm^{-1} peak.

Interestingly, spectral deconvolution indicated the gibbsite-derived WEOM possessed relatively strong metal-OH peaks from 3450 to 3650 cm^{-1} that were not present in the goethite or control samples. This suggests that Al in the gibbsite WEOM was present as some form of $Al(OH)_x$, whereas dissolved Fe in the goethite treatment was present in its elemental form (Fe^{3+}). The asymmetric carboxyl stretch peak area ($\nu_{as}COO^-$) was significantly higher in WEOM from the gibbsite treatment than in the control (gibbsite^a > control^{ab} > goethite^b). Increased carboxyl content is typically associated with increased humification and biodegradation (Stevenson, 1994; Qualls et al., 2003). However, carboxyl groups interact strongly with oxide surfaces via ligand exchange, thereby removing them from

Table 2
Peak assignments for DRIFT spectra of DOM samples.

Peak position (cm)	Assignment	Reference
3530	Metal-OH stretch	Socrates (2001)
3470	Metal-OH stretch	Socrates (2001)
3380	phenolic OH stretch	Gressel et al. (1995), Swift (1996), Baes and Bloom (1989), Senesi and Loffredo (1999)
2990	Aliphatic C–H stretch	Socrates (2001), Colthup (1950)
2970–2950	Aliphatic CH_2 and CH_3 stretching	Gressel et al. (1995), Swift (1996)
2910–2900	Aliphatic C–H stretching	Socrates (2001), Senesi and Loffredo (1999)
1730	symmetric C═O stretch of esters	Swift (1996)
1655–1640	C═O stretch of amides	Gressel et al. (1995), Swift (1996), Baes and Bloom (1989), Senesi and Loffredo (1999)
1580	asymmetric COO^- stretch	Gressel et al. (1995), Swift (1996), Baes and Bloom (1989), Colthup (1950)
1455–1445	CH_2 scissoring	Socrates (2001)
1390–1400	symmetric COO^- stretch	Gressel et al. (1995), Swift (1996), Baes and Bloom (1989), Colthup (1950)
1385	COO-metal stretch	Fu and Quan (2006), Gu et al. (1994)
1270–1235	C–O stretch of polysaccharides, OH deformation of COOH	Stevenson (1994)
1200	C–O stretch of polysaccharides, OH deformation of COOH	Stevenson (1994)
~1140	C–O stretch of polysaccharides	Stevenson (1994)
1080	C–O stretch of polysaccharides	Stevenson (1994)
1055–1040	C–O stretch of polysaccharides	Stevenson (1994)
~950	C–O stretch of polysaccharides	Stevenson (1994)
~900	C–O stretch of polysaccharides	Stevenson (1994)

Table 3
Significant differences of DRIFT peak areas among treatments. Measurements were performed on WEOM solutions.

	Amide I	Amidel/Σpolysaccharide	Metal + COO^-	Esters	$v_{as}COO^-$	vMetal-OH
peak max (cm^{-1})	1650	1650/sum (1240,1140,1055,950,900)	1380	1730	1580	3500, 3530
P-value	0.0018	0.0322	0.0159	0.0067	0.0213	<0.0001
Control	A	A	B	A	AB	B
Goethite	B	B	A	B	B	B
Gibbsite	AB	AB	AB	AB	A	A

Significance was determined using one-way ANOVA by treatment followed by Tukey's HSD *post hoc* test ($a = 0.05$). Within each column, different letters indicate statistically significant differences among variables. ($n = 7$) for each treatment.

solution. Therefore, lower carboxyl content in the goethite WEOM may indicate greater carboxylate bonding to oxide surfaces, analogous to the greater metal-carboxyl bonding noted above.

Several time dependent trends in the DRIFT spectra were shared by all treatments (Fig. 2). In general, the amide I peak area increased and the polysaccharide peak area showed a slight decrease over time, consistent with increasing protein:polysaccharide ratios in WEOM. The carboxyl:polysaccharide ratio exhibited a general decline over time.

3.6. TG-DTA

All observable DTA peaks were exotherms, and all exotherms were associated with mass loss. In general, DTA curves were composed of three peaks with maxima around 300 °C (Exo_1), 410 °C (Exo_2) and 550 °C (Exo_3), though goethite-derived WEOM curves showed a general merging of Exo_2 and Exo_3 peaks with increasing time of incubation (Fig. 3 and Table 4). Because Exo_2 and Exo_3 peaks merged, mass loss and enthalpies were calculated for the sum of the Exo_2 and Exo_3 peaks in the goethite treatment. In all treatments, peaks in higher temperature ranges released more energy per unit mass than peaks in lower temperature ranges, which is consistent with previous research showing that more recalcitrant, higher-energy compounds are associated with higher combustion temperatures (cf. Plante et al., 2009). Distribution of mass loss among the three peaks varied both among treatments and over time, but quantitative comparisons are difficult due to the merging of peaks in curves from the goethite treatment. This merging of peaks could be the result of differences in the molecular composition of goethite-derived WEOM relative to control or gibbsite-derived WEOM. However, previous studies indicate that peak position and shape can also be affected by

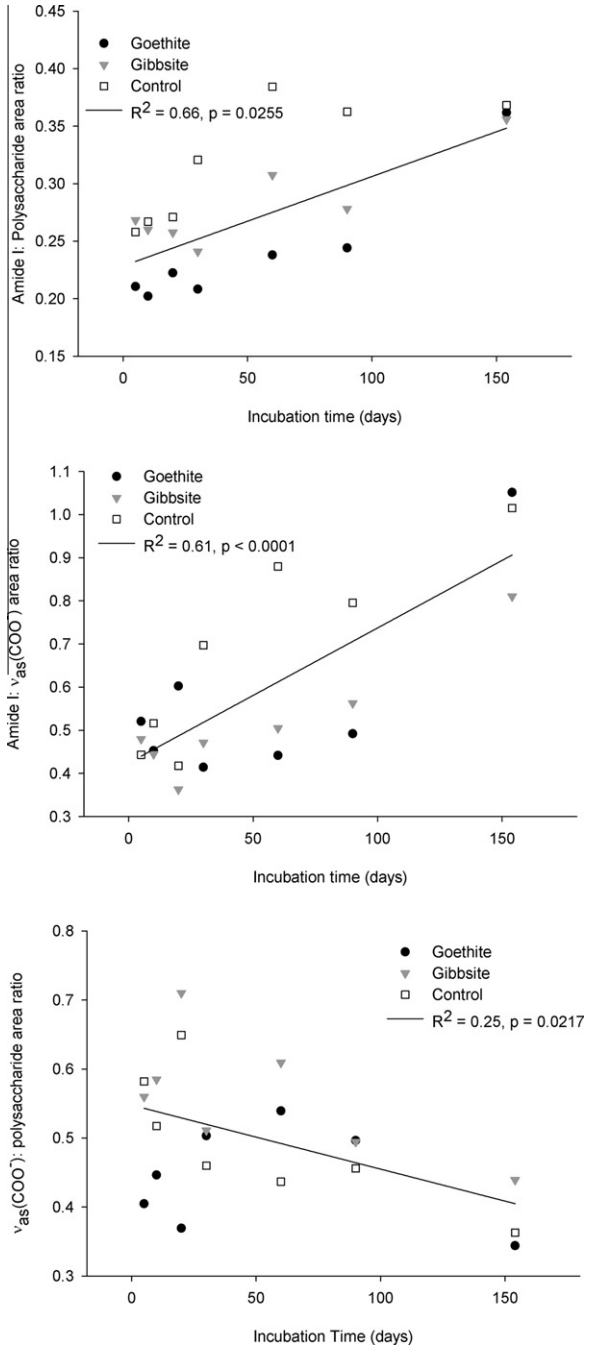

Fig. 2. Analysis of DRIFT spectra of WEOM solutions. The ratio of the areas under the polysaccharide, amide 1, and the asymmetric carboxyl peak are plotted against time. (a) The ratio of area under the Amide 1 band and polysaccharide peak are plotted against time of incubation, showing a general increase in amides over time in all treatment groups. (b) The ratio of area under the Amide 1 band and the asymmetric carboxyl peak are plotted against time of incubation, showing an enrichment in amides in comparison to carboxyls with increasing time of incubation. (c) The ratio of area under the asymmetric carboxyl peak and the area under the polysaccharide peak are plotted against time of incubation showing a slight decrease in carboxyl content in comparison to polysaccharide content with increasing time of incubation.

humus-complexing metals (Provenzano and Senesi, 1998). Prior studies indicate that the presence of organo-Fe(III) complexes lowers the initiation temperature of DTA peaks, while organo-Al bonding tends to increase them (Schnitzer and Kodama, 1972; Tan, 1978; Lu et al., 1997). Though organo-metal complexes were certainly present in the WEOM solutions, metal:C ratios were several orders of magnitude smaller than those shown previously to effect initialization temperatures (Table 1). Also, when mass and energy losses from goethite-derived WEOM Exo_2 and Exo_3 peaks were separated using basic peak decomposition, enthalpies of the two peaks were very similar, indicating the compounds combusting in Exo_2 and Exo_3 were similar in composition. These data indicate that merging of Exo_2 and Exo_3 peaks was more likely the result of actual changes in WEOM composition rather than the presence of small amounts of organo-metal complexes.

In general, combustion in specific temperature ranges has been associated with the breakdown of specific compound types (Dell'Abate et al., 2002; Lopez-Capel et al., 2005, 2006; Manning et al., 2005; Plante et al., 2005; Montecchio et al., 2006). However the assignment of specific compounds to certain temperature ranges in DTA profiles varies widely. Peaks at ~300 °C can be produced by combustion of polysaccharides, decarboxylation of acidic groups, and dehydration of hydroxylate aliphatic structures (Ciavatta et al., 1991; Dell'Abate et al., 2002). Peaks at ~400 °C have been associated with the combustion of plant and microbially-derived aliphatic structures (Sheppard and Forgeron 1987; Schulten and Leinweber, 1999), but are sometimes assigned to aromatics (Ranalli et al., 2001; Dell'Abate et al., 2002; Strezov et al., 2004). Peaks around ~500–550 °C have also been associated with combustion of aromatic structures and cleavage of C–C bonds (Stevenson, 1994; Montecchio et al., 2006). However, other studies assign combustion at temperatures over 500 °C to polycondensed aromatics such as char or black C (Almendros et al., 1982; Lopez-Capel et al., 2005; De la Rosa et al., 2008). Though previous studies have shown good agreement between combustion at temperatures >500 °C and the abundance of aromatics and polycondensed aromatics, DRIFT spectra of the WEOM did not indicate a large abundance of aromatics (spectra lack the characteristic prominent peak at 1500 cm^{-1} that is indicative of aromatics). This may indicate that mass losses at ~550 °C were actually the result of cleavage of unsaturated C–C bonds sourced from non-aromatic compounds. Also, assignment of mass loss at certain temperatures cannot be definitively attributed to any particular structural quality, due to both the heterogeneity of natural organic substances and the fact that peak temperatures have been known to vary with a variety of experimental parameters (Cebulak and Langier-Kùzniarowa, 1997).

WEOM from all treatments had relatively low enthalpy of combustions values, averaging 9.4 kJ g^{-1} of total lyophilized mass. WEOM from the goethite treatment exhibited the greatest enthalpy of combustion based both on total sample weight and mass loss during combustion (Table 4). Average enthalpy of WEOM, as measured in kJ per g of mass loss, was significantly higher in the goethite treat-

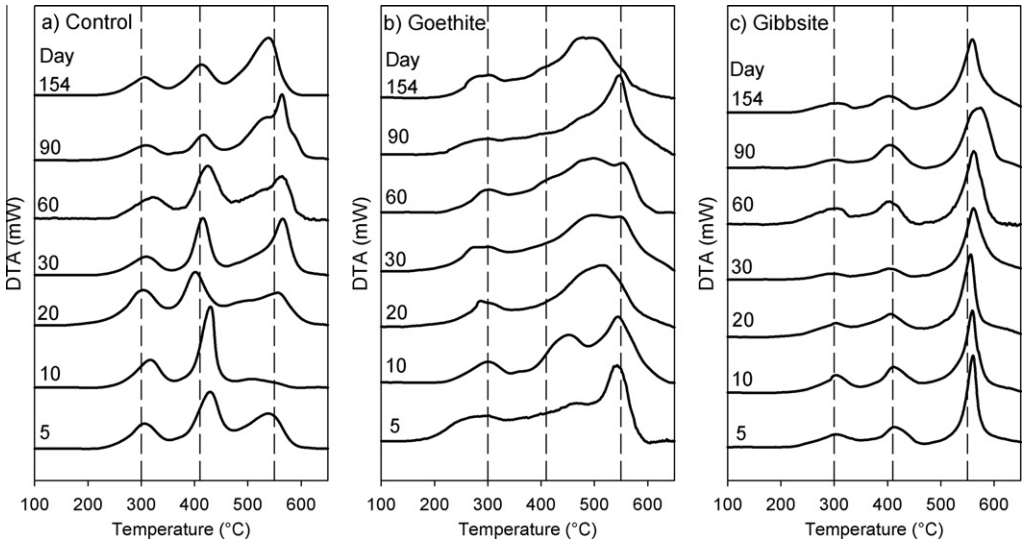

Fig. 3. DTA plots for WEOM from each treatment at each sampling time during the incubation. (a) Control treatment: quartz sand and forest floor material, (b) Goethite treatment: quartz sand mixed with goethite and forest floor material, (c) Gibbsite: quartz sand mixed with gibbsite and forest floor material. Drop lines represent average peak maximums: 300 °C, 410 °C, and 550 °C. DTA curves were normalized prior to graphing to facilitate comparison among plots.

ment than in either the control or the gibbsite treatment ($p = 0.0198$), suggesting that exposure to goethite increased the energy content of WEOM.

4. DISCUSSION

The results of this study indicate that interaction with goethite and gibbsite surfaces influenced both the quantity and quality of WEOM produced during active biodegradation of forest floor organic material. Previous research demonstrated that interaction with mineral surfaces results in systematic fractionation of WEOM by molecular size and type into adsorbed and dissolved pools in both abiotic batch (Zhou et al., 2001; Chorover and Amistadi, 2001) and column (Guo and Chorover, 2003) experiments. Previous studies also documented decreases in both WEOM abundance and biodegradability as the result of exposure to mineral matrices (Kalbitz et al., 2000; Schwesig et al., 2003; Kalbitz et al., 2005). Consistent with this prior research, our data indicate that exposure to goethite and gibbsite surfaces reduced concentrations of dissolved organic C and also significantly changed its molecular composition and energetics.

4.1. Influence of goethite and gibbsite surfaces on WEOM molecular characteristics

Goethite and gibbsite surface sorption processes differed in their effect on WEOM properties, with both molecular composition and thermal stability varying with treatment. Goethite-treatment derived WEOM and gibbsite-treatment derived WEOM varied in their molecular and thermal characteristics, and both displayed qualities significantly different from quartz-treatment derived WEOM.

In general, WEOM from the goethite treatment was depleted in fatty acids and proteins relative to the control treatment, but also had a significantly lower abundance of carboxylated components than the gibbsite treatment. Considering these data along with information from the TG and DTA profiles indicating that the majority of mass and energy loss occurred over the temperature range of 400–550 °C, WEOM from the goethite treatment appeared to be dominated by aliphatics and carbohydrates of mid-to-high-range thermal stability. WEOM from the goethite treatment exhibited higher average enthalpy than that from either the gibbsite or control treatments, suggesting that interaction with goethite surfaces significantly increased the thermal and, by extension, possibly the biological stability of WEOM. The translation of thermal stability to biological recalcitrance has not been firmly established. However, indices of thermal stability have shown good agreement with other traditional indices of humification (Ciavatta et al., 1990; Plante et al., 2009). Therefore, enthalpy data may suggest that exposure to goethite surfaces increases the apparent biological stability of WEOM. WEOM from the control treatment exhibited a higher overall mass loss during combustion than WEOM from the oxide treatments, though the difference was only significant between goethite and control treatments ($p = 0.0142$). Lower mass loss values for the goethite WEOM may indicate a greater abundance of compounds with high thermal stability, but may also be partially accounted for by the presence of Fe in these samples which would contribute to the ash content.

DRIFT data indicated that molecular composition of WEOM from the gibbsite treatments was similar to WEOM from the control treatments, aside from having a higher carboxyl content. Furthermore, the TG/DTA data suggested that WEOM from the gibbsite treatment was dominated by high temperature, high enthalpy organics. The abundance of thermally stable components along with high carboxyl content may suggest a more advanced degree of

Table 4
TG/DTA analysis of water extractable organic matter solutions. Values indicate changes in the distribution of mass and energy loss over the course of the incubation.

Treatment	Incubation length	Enthalpy		EXO_{Tot} % mass loss	% of total mass loss per peak			Enthalpy (kJ $g_{mass\ loss}^{-1}$)		
	Days	kJ $g_{mass\ loss}^{-1}$	kJ g_{mass}^{-1}		Exo_1	Exo_2	Exo_3	Exo_1	Exo_2	Exo_3
Control	5	21.7	11.4	52	49	34	18	9.9	25.7	46.3
	10	21.7	10.2	47	55	32	13	13.2	37.4	19.3
	20	23.2	12.0	52	50	29	21	13.4	19.5	51.8
	30	8.1	7.7	95	19	71	10	7.6	3.3	42.7
	60	14.3	7.4	52	50	25	25	5.8	21.4	24.4
	90	8.2	8.1	99	15	71	14	8.0	2.2	38.5
	154	19.2	9.6	50	52	14	34	5.6	42.4	30.1
	Average over time	16.6 (2.4)	9.5 (0.7)	64(9)	41 (6)	39 (8)	19 (3)	9.1 (1.2)	21.7 (5.8)	36.1 (4.5)
						Exo_2+Exo_3			Exo_2+Exo_3	
Goethite	5	32.0	15.0	46	47	53		21.9	42.3	
	10	17.9	8.5	48	46	54		5.5	28.3	
	20	23.8	11.4	47	48	52		15.4	32.4	
	30	20.5	9.3	45	52	48		6.5	36.5	
	60	20.7	8.3	39	48	52		5.7	36.2	
	90	22.9	9.6	47	43	57		13.4	25.9	
	154	25.1	9.5	37	43	57		9.2	38.1	
	Average over time	23.2 (1.7)	10.2 (0.9)	44(2)	47(1.2)	46 (1)		11.1 (2.3)	34.2 (2.2)	
Gibbsite	5	17.0	9.4	55	48	25	28	6.1	13.9	38.2
	10	17.6	10.0	57	44	26	29	6.6	15.3	36.0
	20	20.5	11.0	54	44	25	31	8.1	17.4	40.8
	30	14.5	8.2	57	37	25	38	3.1	10.6	28.2
	60	15.4	8.0	52	42	24	33	4.8	7.4	34.7
	90	11.9	5.9	49	42	26	33	3.3	10.6	24.0
	154	14.9	6.9	46	44	24	32	3.7	9.8	34.0
	Average over time	16.0 (1.0)	8.5 (0.7)	52 (1)	43 (1)	25 (0)	32 (1)	5.1 (0.7)	12.2(1.3)	33.7(2.2)

Numbers in parentheses the standard errors for the 7 sampling times.

biodegradation for WEOM from the gibbsite treatment in comparison to the control (Ciavatta et al., 1990; Stevenson, 1994; Qualls et al., 2003). This apparent advanced degree of biodegradation could be the result of differences in the abundance and bioavailability of dissolved organic C, or the result of preferential sorption of more thermally labile organics by gibbsite surfaces.

Ultraviolet–visible spectroscopic indices of WEOM quality were less conclusive. Molar absorptivity indicated a general increase in aromaticity over time in all treatments, a phenomenon often observed with increasing biodegradation (Stevenson, 1994). However, aromaticity of WEOM from the oxide treatments was not statistically different than control WEOM. This may be due to preferential sorption of aromatic compounds by oxide surfaces as suggested by differences in apparent molar mass among treatments.

The observation that apparent molar mass data were significantly affected by the presence of dissolved metals in the WEOM solutions is consistent with the emerging paradigm of WEOM as being comprised of aggregated molecular entities inter-bonded by bridging cations as well as through H-bonding and hydrophobic interaction (Sutton and Sposito, 2005). Apparent molar mass was strongly correlated with Fe:C and Al:C ratios in the oxide treatments, suggesting that formation of metal-humus complexes strongly affected the apparent molar mass of WEOM. Even though Mw_{APP} of WEOM from the oxide treatments was likely increased by bonding with metals, WEOM from the goethite treatment still had significantly lower Mw_{APP} than the control ($p = 0.0024$) while WEOM from the gibbsite treatment had intermediate Mw_{APP} values. These data suggest the preferential sorption of high molecular weight compounds by goethite surfaces, consistent with previous research (Chorover and Amistadi, 2001; Omoike and Chorover, 2006; Hunt et al., 2007; Ohno et al., 2007). Contrary to previous research (Peuravuori and Pihlaja, 1997; Guo and Chorover, 2003), E_2:E_3 values were not correlated with Mw_{APP}, either before or after accounting for the influence of dissolved metal concentrations on Mw_{APP}. Differences in E_2:E_3 may therefore indicate differences in the abundance of conjugated bonds associated with chromophores, with goethite having a significantly higher abundance of chromophores than both the control and gibbsite treatments.

4.2. Metal-humus complex formation and abundance

Dissolved Fe and Al were present in WEOM from all treatments, and DRIFT data indicated that these dissolved metals interacted with organics in solution. Concentrations of both Fe, in goethite-derived WEOM solutions, and Al, in gibbsite-derived WEOM solutions were several orders of magnitude larger than the total inorganic concentrations predicted from respective solubility constants. This large increase in aqueous concentration was likely due to the presence of low molecular weight organic acids that increased the extent of oxide solubilization via ligand-promoted dissolution and aqueous metal-ligand complex formation (Stevenson, 1967; Zunino and Martin, 1977; Robert and Berthelin, 1986; Tan, 1986; Pohlman and McColl, 1988; Essington et al., 2005). Metal:C values were lower than values found to induce precipitation of metal-humus complexes (Nierop et al., 2002), so any such complexes formed during the incubation likely remained in solution.

Just as goethite and gibbsite surfaces differed in their effects on WEOM properties, aqueous Al and Fe also differed in their interaction with WEOM. The larger area of the 1380 cm^{-1} peak in the DRIFT spectra indicated that dissolved Fe had a greater propensity for metal-ligand complexation reactions with dissolved organics than dissolved Al. DRIFT spectra suggest that organic complexed Al was at least partially hydrolyzed, and most likely formed metal-humus complexes both in the form of Al-organic and $Al(OH)_x$-organic complexes. DRIFT spectra did not show evidence of hydroxy-Fe species.

4.3. Transition of WEOM properties with increasing time of incubation

Data did not indicate that the influence of oxide surfaces on WEOM properties varied with increasing time of incubation, but rather that oxide surfaces had a continuous and consistent effect on WEOM properties throughout the biodegradation process. Previous work has indicated that sorption reactions between oxide surfaces and dissolved organics proceed rapidly, and that the strength of sorption increases over time (Kaiser et al., 2007). Once bonds are formed, desorption of organics displays a strong hysteresis relative to adsorption indicating that organics are tightly sorbed to the oxide surface (Gu et al., 1994). Therefore, we speculate that changes in WEOM composition throughout the biodegradation process were indicative of changes in microbial activity, microbial turnover, and the removal of organics from solution by sorption processes. Data did suggest a general transition from plant-based compounds to microbially-sourced products in all treatments (an enrichment in microbial products with increasing degree of biodegradation), a trend previously noted by Kalbitz et al. (2003b).

Both DRIFT and TG/DTA data supported the idea of a transition from plant-based compounds to microbially-derived compounds in WEOM solutions over time. Protein:polysaccharide ratios increased over time in all treatments, while the carboxyl:polysaccharide values exhibited a general decline. We interpret the increase in protein:polysaccharide as indicating enrichment of WEOM in microbial byproducts concomitant with consumption of plant-derived products over time. Polysaccharides derive from both plant and microbial sources, and the ratio of carboxyl groups to polysaccharides was likely affected both by the degree of decomposition of the plant-based organics and the abundance of biomolecules added to the WEOM through biomass turnover. The negative carboxyl:polysaccharide trend thus supports the notion that the WEOM transitioned from dominantly plant-derived to dominantly microbial-derived biomolecules over time. In addition, all treatments exhibited an increase in protein:carboxyl ratio that also indicates an increased dominance of WEOM by microbially-derived biomolecules.

WEOM from all treatments had relatively low enthalpy values, averaging 9.4 kJ g^{-1} across all treatments. These values are slightly lower than values for bulk soil organic

matter and humic acids found in the literature, which typically range from 12 to 20 kJ g^{-1} (Peuravuori et al., 1999; Rovira et al., 2008; Rasmussen and White, 2010), indicating that WEOM has a relatively low enthalpy of combustion in comparison to soil organic matter as a whole. The low enthalpy of WEOM is consistent with previous research indicating that WEOM is one of the more biologically labile fractions of soil organic matter (Zsolnay, 1996). The enthalpies of Exo_1, Exo_2 and Exo_3 varied according to treatment (Table 4), indicating variation in the materials combusting at each temperature range. This is consistent with results from the DRIFT analysis that indicated both differences in the molecular composition of WEOM among treatments and transition of WEOM composition with increasing time of incubation.

5. SUMMARY

Results of this experiment illustrate that interaction with goethite and gibbsite surfaces induced significant changes in the molecular composition, thermal properties and reactivity of water extractable organic matter produced during the active biodegradation of forest floor organic material. These data support previous work indicating that the mineral matrix has a strong influence on WEOM properties, and also indicate that specific mineral phases lead to significantly different effects on WEOM properties. Such changes in WEOM composition are important to soil C cycling as a whole, since the dissolved fraction of soil organic matter comprises the largest flux of nutrients to subsurface soils in temperate forested systems. Changes in the properties of dissolved organics therefore have the potential to affect soil respiration rates and possibly microbial community composition and abundance. In addition, since introduction of labile dissolved organics to subsurface soils often has a priming effect (i.e., increasing the biodegradation of old/stable C pools), changes in WEOM properties may affect turnover rates of older/stable C pools in subsurface soils as well. Thus incorporation of mineral data has the potential to improve both our understanding of soil C cycling and current modeling of soil C dynamics.

ACKNOWLEDGEMENTS

This work was supported by a Grant from the National Science Foundation (DEB 0543130). Many thanks to Dr. Mary Kay Amistadi and Selene Hernandez Ruiz for their generous assistance with HPLC and ICP-MS measurements and Dr. Mercer Meding for his expert guidance and assistance with TG/DTA measurements. The authors would also like to thank Dr. Jack Middelburg and two anonymous reviewers for their thoughtful edits and suggestions which greatly improved the quality of this paper.

REFERENCES

Amundson R. (2001) The carbon budget in soils. *Annu. Rev. Earth Planet. Sci.* **29**, 535–562.

Almendros G., Polo A. and Vizcayno C. (1982) Application of thermal analysis to the study of several Spanish peats. *J. Therm. Anal.* **24**, 175–182.

Baes A. U. and Bloom P. R. (1989) Diffuse reflectance and transmission Fourier transform infrared spectroscopy of humic and fulvic acids. *Soil Sci. Am. J.* **53**, 695–700.

Baldock J. A. and Skjemstad J. O. (2000) Role of the soil matrix and minerals in protecting natural organic materials against biological attack. *Organ. Geochem.* **31**, 697–710.

Boudot J. P., Bel Hadj B. A., Steiman R. and Seigle-Murandi F. (1989) Biodegradation of synthetic organo-metallic complexes of iron and aluminum with selected metal:C ratios. *Soil Biol. Biochem.* **21**, 961–966.

Brunauer S., Emmett P. H. and Teller E. (1938) Adsorption of gases in multimolecular layers. *J. Am. Chem. Soc.* **60**, 309–319.

Byler D. M., Gerasimowicz W. V., Susi H. and Schnitzer M. (1987) FT-IR spectra of soil constituents: fulvic acid and fulvic acid complex with ferric ions. *Appl. Spectrosc.* **41**(8), 1428–1430.

Cassel D. K. and Nielsen D. R. (1986) Field capacity and available water capacity. In *Methods of Soil Analysis. Part 1: Physical and Mineralogical Methods, second ed. SSSA Book Series 5* (ed. A. Klute). SSSA Inc., Madison, WI, pp. 901–926.

Chin Y. P., Aiden G. and O'Loughlin E. (1994) Molecular weight, polydispersity, and spectroscopic properties of aquatic humic substances. *Environ. Sci. Technol.* **28**, 1853–1858.

Chorover J. and Amistadi M. K. (2001) Reaction of forest floor organic matter at goethite, birnessite and smectite surfaces. *Geochim. Cosmochim. Acta* **65**(1), 95–109.

Cebulak S. and Langier-Kùzniarowa A. (1997) Application of oxyreactive thermal analysis to the examination of organic matter associated with rocks. *J. Therm. Anal. Calorim.* **50**(1–2), 175–190.

Ciavatta C., Govi M., Antisari L. V. and Sequi P. (1990) Characterization of humified compounds by extraction and fractionation on solid polyvinylpyrrolidone. *J. Chromatogr.* **509**(1), 141–146.

Ciavatta C., Govi M., Antisari L. V. and Sequi P. (1991) Determination of organic carbon in aqueous extracts of soils and fertilizers. *Commun. Soil Sci. Plant. Anal.* **22**, 795–807.

Colthup N. B. (1950) Spectra-structure correlations in the infra-red region. *J. Opt. Soc. Am.* **40**(6), 397–400.

Cornell R. M. and Schwertmann U. (1996) *The Iron Oxides*. VCH Inc., New York.

De la Rosa J. M., Knicker H., Lopez-Capel E., Manning D. A. C., Gonzalez-Perez J. A. and Gonzalez-Vila F. J. (2008) Direct detection of black carbon in soils by Py-GC/MS, carbon-13 NMR spectroscopy and thermogravimetric techniques. *Soil Sci. Soc. Am. J.* **72**, 258–267.

Dell'Abate M. T., Benedetti A., Trinchera A. and Dazzi C. (2002) Humic substances along the profile of two typic haploxerert. *Geoderma* **107**, 281–296.

Essington M. E., Nelson J. B. and Holden W. L. (2005) Gibbsite and goethite solubility: The influence of 2-ketogluconate and citrate. *Soil Sci. Soc. Am. J.* **69**, 996–1008.

Eusterhues K., Rumpel C., Kleber M. and Kögel-Knabner I. (2003) Stabilization of soil organic matter by interactions with minerals as revealed by mineral dissolution and oxidative degradation. *Org. Geochem.* **34**, 1591–1600.

Evanko C. R. and Dzombak D. A. (1999) Surface complexation modeling of organic acid sorption to goethite. *J. Colloid Interface Sci.* **214**, 189–206.

Fu H. and Quan X. (2006) Complexes of fulvic acid on the surface of hematite, goethite, and akaganeite: FTIR observation. *Chemosphere* **63**, 403–410.

Greenland D. J. (1971) Interactions between humic and fulvic acids and clays. *Soil Sci.* **111**, 34.

Gressel N., McGrath A. E., McColl J. G. and Powers R. F. (1995) Spectroscopy of aqueous extracts of forest litter I: suitability of methods. *Soil Sci. Soc. Am. J.* **59**, 1715–1723.

Gu B., Schmitt J., Chen Z., Liang L. and McCarthy J. F. (1994) Adsorption and desorption of natural organic matter on iron oxide: mechanisms and models. *Environ. Sci. Technol.* **28**, 38–46.

Guan X.-H., Shang C. and Chen G.-H. (2006) ATR-FTIR investigation of the role of phenolic groups in the interaction of some NOM model compounds with aluminum hydroxide. *Chemosphere* **65**, 2074–2081.

Guo M. and Chorover J. (2003) Transport and fractionation of dissolved organic matter in soil columns. *Soil Sci.* **168**, 108–118.

Heckman K., Welty-Bernard A., Rasmussen C. and Schwartz E. (2009) Geologic controls of soil carbon cycling and microbial dynamics in temperate conifer forests. *Chem. Geol.* **267**, 12–23.

Hunt J. F., Ohno T., He Z., Honeycutt C. W. and Dail D. B. (2007) Influence of decomposition on chemical properties of plant- and manure-derived dissolved organic matter and sorption to goethite. *J. Environ. Qual.* **36**, 135–143.

Jones D. L. and Edwards A. C. (1998) Influence of sorption on the biological utilization of two simple carbon substrates. *Soil Biol. Biochem.* **30**, 1895–1902.

Kaiser K. and Guggenberger G. (2000) The role of DOM sorption to mineral surfaces in the preservation of organic matter in soils. *Org. Geochem.* **31**, 711–725.

Kaiser K. and Zech W. (2000) Dissolved organic matter sorption by mineral constituents of subsoil clay fractions. *J. Plant Nutr. Soil Sci.* **163**, 531–535.

Kaiser K., Mikutta R. and Guggenberger G. (2007) Increased stability of organic matter sorbed to ferrihydrite and goethite on aging. *Soil Sci. Soc. Am. J.* **71**, 711–719.

Kalbitz K., Solinger S., Park J.-H., Michalzik B. and Matzner E. (2000) Controls on the dynamics of dissolved organic matter in soils: a review. *Soil Sci.* **165**, 277–304.

Kalbitz K., Schmerwitz J., Schwesig D. and Matzner E. (2003a) Biodegradation of soil-derived dissolved organic matter as related to its properties. *Geoderma* **113**, 273–291.

Kalbitz K., Schwesig D., Schmerwitz J., Kaiser K., Haumaier L., Glaser B., Ellerbrock R. and Leinweber P. (2003b) Changes in properties of soil-derived dissolved organic matter induced by biodegradation. *Soil Biol. Biochem.* **35**, 1129–1142.

Kalbitz K., Schwesig D., Rethemeyer J. and Matzner E. (2005) Stabilization of dissolved organic matter by sorption to the mineral soil. *Soil Biol. Biochem.* **37**, 1319–1331.

Kampf N., Scheinost A. L. and Schulze D. G. (2000) Oxide minerals. In *Handbook of Soil Science* (ed. M. E. Sumner). CRC Press, Boca Raton, FL, pp. 125–168.

Lindsay W. L. (1997) *Chemical Equilibria in Soils*. John Wiley & Sons, New York.

Lopez-Capel E., Sohi S. P., Gaunt J. L. and Manning D. A. C. (2005) Use of thermogravimetry differential scanning calorimetry to characterize modelable soil organic matter fractions. *Soil Sci. Soc. Am. J.* **69**, 136–140.

Lopez-Capel E., Abbott G. D., Thomas K. M. and Manning D. A. C. (2006) Coupling of thermal analysis with quadrupole mass spectrometry and isotope ratio mass spectrometry for simultaneous determination of evolved gases and their carbon isotopic composition. *J. Anal. Appl. Pyrolysis* **75**, 82–89.

Lu X. G., Vassallo A. M. and Johnson W. D. (1997) Thermal stability of humic substances and their metal forms: an investigation using FTIR emission spectroscopy. *J. Anal. Appl. Pyrolysis* **43**, 103–113.

Manning D. A. C., Lopez-Capel E. and Barker S. (2005) Seeing soil carbon: use of thermal analysis in the characterization of soil C reservoirs of differing stability. *Mineral. Mag.* **6**, 425–435.

Martin J. P. and Haider K. (1986) Influence of mineral colloids on turnover rates of soil organic carbon. *Soil Sci. Soc. Am. J.* **17**, 283–304.

Masiello C. A., Chadwick O. A., Southon J., Torn M. S. and Harden J. W. (2004) Weathering controls on mechanisms of carbon storages in grassland soils. *Global Biogeochem. Cycles* **18**, GB4023, doi:10.1029/2004GB002219.

Marschner B., Brodowski S., Dreves A., Gleixner G., Gude A., Gootes P. M., Hamer U., Heim A., Jandl G., Ji R., Kaiser K., Kalbitz K., Kramer C., Leinweber P., Rethemeyer J., Schäffer A., Schmidt M. W. I., Schwark L. and Wiesenberg G. L. B. (2008) How relevant is recalcitrance for the stabilization of organic matter in soils?. *J. Plant Nutr. Soil Sci.* **171** 91–110.

McKnight D. M., Bencala K. E., Zellweger G. W., Aiken G. R., Feder G. L. and Thorn K. A. (1992) Sorption of dissolved organic-carbon by hydrous aluminum and iron-oxides occurring at the confluence of deer creek with the Snake River, Summit County. *Colorado. Environ. Sci. Technol.* **26**, 1388–1396.

Meier M., Namjesnik-Dejanovic K., Maurice P. A., Chin Y.-P. and Aiken G. R. (1999) Fractionation of aquatic natural organic matter upon sorption to goethite and kaolinite. *Chem. Geol.* **157**, 275–284.

Michalzik B., Kalbitz K., Park J. H., Solinger S. and Matzner E. (2001) Fluxes and concentrations of dissolved organic carbon and nitrogen – a synthesis for temperate forests. *Biogeochemistry* **52**, 173–205.

Mikutta R., Kleber M., Torn M. S. and Jahn R. (2006) Stabilization of soil organic matter: association with minerals or chemical recalcitrance? *Biogeochemistry* **77**, 25–56.

Mikutta R., Mikutta C., Kalbitz K., Scheel T., Kaiser K. and Jahn R. (2007) Biodegradation of forest floor organic matter bound to minerals via different binding mechanisms. *Geochim. Cosmochim. Acta* **71**, 2569–2590.

Molis E., Barrès O., Marchand H., Sauzéat E., Humbert B. and Thomas F. (2000) Initial steps of ligand-promoted dissolution of gibbsite. *Colloid Surface A* **163**, 283–292.

Montecchio D., Francioso O., Carletti P., Pizzeghello D., Chersich S., Previtali F. and Nardi S. (2006) Thermal analysis (TG-DTA) and DRIFT spectroscopy applied to investigate the evolution of humic acids in forest soil at different vegetation stages. *J. Therm. Anal. Calorim.* **83**, 393–399.

Nierop K. G. J., Jansen B. and Verstraten J. M. (2002) Dissolved organic matter, aluminum and iron interactions: precipitation induced by metal/carbon ratio, pH and competition. *Sci. Total Environ.* **300**, 201–211.

Nierop K. G. J., Naafs D. F. W. and Verstraten J. M. (2003) Occurrence and distribution of ester-bond lipids in Dutch coastal dune soils along a pH gradient. *Org. Geochem.* **34**, 719–729.

Ohno T., Chorover J., Omoike A. and Hunt J. (2007) Molecular weight and humification index as predictors of adsorption for plant- and manure-derived dissolved organic matter to goethite. *Eur. J. Soil Sci.* **58**, 125–132.

Omoike A. and Chorover J. (2006) Adsorption to goethite of extracellular polymeric substances from *Bacillus subtilis*. *Geochim. Cosmochim. Acta* **70**, 827–838.

Parfitt R. L., Fraser A. R. and Farmer V. C. (1977) Adsorption on hydrous oxides. III. Fulvic acid and humic acid on goethite, gibbsite and imogolite. *Eur. J. Soil Sci.* **28**, 289–296.

Plankey B. J. and Patterson H. H. (1987) Kinetics of aluminum-fulvic acid complexation in acidic waters. *Environ. Sci. Technol.* **21**, 595–601.

Plante A. F., Pernes M. and Chenu C. (2005) Changes in clay-associated organic matter quality in a C depletion sequence as measured by differential thermal analyses. *Geoderma* **129**, 186–199.

Plante A. F., Fernández J. M. and Leifeld J. (2009) Application of thermal analysis techniques in soil science. *Geoderma* **153**, 1–10.

Peuravuori J. and Pihlaja K. (1997) Molecular size distribution and spectroscopic properties of aquatic humic substances. *Anal. Chim. Acta* **337**, 133–149.

Peuravuori J., Paaso N. and Pihlaja K. (1999) Kinetic study of the thermal degradation of lake aquatic humic matter by thermogravimetric analysis. *Thermochim. Acta* **325**, 181–193.

Pohlman A. A. and McColl J. G. (1988) Soluble organics from forest litter and their role in metal dissolution. *Soil Sci. Soc. Am. J.* **52**, 265–271.

Provenzano M. R. and Senesi N. (1998) Differential scanning calorimetry of river aquatic fulvic acids and their metal complexes. *Fresenius Environ. Bull.* **7**, 423–428.

Theng B. K. G. and Tate K. R. (1989) Interactions of clays with soil organic constituents. *Clay Res.* **8**, 1–10.

Qualls R. G., Takiyama A. and Wershaw R. L. (2003) Formation and loss of humic substances during decomposition in a pine forest floor. *Soil Sci. Soc. Am. J.* **67**, 899–909.

Ranalli G., Bottura G., Taddei P., Marchetti R. and Sorlini C. (2001) Composting of solid and sludge residues from agricultural and food industries. Bioindicators of monitoring and compost maturity. *J. Environ. Sci. Heal. A* **36**, 415–436.

Rasmussen C. and White, II, D. A. (2010) Vegetation effects on soil organic carbon quality in an arid hyperthermic ecosystem. *Soil Sci.* **175**, 438–446.

Robert M. and Berthelin J. (1986) Role of biological and biochemical factors in soil mineral weathering. In *Interaction of Soil Minerals with Natural Organics and Microbes, Special Publication 17* (eds. P. M. Huang and M. Schnitzer). Soil Science Society of America, Madison, pp. 1–27.

Rovira R., Kurz-Besson C., Couteaux M. M. and Vallejo V. R. (2008) Changes in litter properties during decomposition: a study by differential thermogravimetry and scanning calorimetry. *Soil Biol. Biochem.* **40**, 172–185.

Rumpel C. and Kögel-Knabner I. (2010) Deep soil organic matter – a key but poorly understood component of terrestrial C cycle. *Plant Soil*, doi: 10.1007/s11104-010-0391-5.

Scheel T., Dörfler C. and Kalbitz K. (2007) Precipitation of dissolved organic matter by aluminum stabilizes carbon in acidic forest soils. *Soil Sci. Soc. Am. J.* **71**, 64–74.

Schnitzer M. and Kodama H. (1972) Differential thermal analysis of metal-fulvic acid salts and complexes. *Geoderma* **7**, 93–103.

Schulten H. R. and Leinweber P. (1999) Thermal stability and composition of mineral-bound organic matter in density fractions of soil. *Eur. J. Soil Sci.* **50**, 237–248.

Schwertmann U. (1991) Solubility and dissolution of iron oxides. *Plant Soil* **130**, 1–25.

Schwesig D., Kalbitz K. and Matzner E. (2003) Mineralization of dissolved organic carbon in mineral soil solution of two forest soils. *J. Plant Nutr. Soil Sci.* **166**, 585–593.

Senesi N. and Loffredo E. (1999) The chemistry of soil organic matter. In *Soil Physical Chemistry, second ed.* (ed. D. L. Sparks). CRD Press LLC, New York, pp. 239–370.

Sheppard J. D. and Forgeron D. W. (1987) Differential thermogravimetry of peat fractions. *Fuel* **66**, 232–236.

Socrates G. (2001) *Infrared and Raman Characteristic Group Frequencies: Tables and Charts Third Edition*. John Wiley & Sons Ltd., New York.

Stevenson F. J. (1967) Organic acids in soils. In *Soil Biochemistry* (eds. A. D. McLaren and G. H. Peterson). Marcel Dekker, New York, pp. 119–146.

Stevenson F. J. (1994) *Humus Chemistry – Genesis, Composition, Reactions*, second ed. Wiley, New York.

Stevenson F. J. and Cole M. A. (1999) *Cycles of Soil: Carbon, Nitrogen, Phosphorous, Sulfur, Micronutrients*, second ed. John Wiley & Sons, Inc., New York.

Strezov V., Moghtaderi B. and Lucas J. A. (2004) Computational calorimetric investigation of the reactions during thermal conversion of wood biomass. *Biomass Bioenerg.* **27**, 459–465.

Sutton R. and Sposito G. (2005) Molecular structure in soil humic substances: the new view. *Environ. Sci. Technol.* **39**, 9009–9015.

Swift R. S. (1996) Organic matter characterization. In *Methods of Soil Analysis: Part 3, Chemical Methods, SSSA Book Series 5* (ed. D. L. Sparks et al.). Soil Science Society of America, Madison, WI, pp. 1018–1020.

Tan K. H. (1978) Formation of metal–humic acid complexes by titration and their characterization by differential thermal analysis and infrared spectroscopy. *Soil Biol. Biochem.* **10**, 123–129.

Tan K. H. (1986) Degradation of soil minerals by organic acids. In *Interaction of Soil Minerals with Natural Organics and Microbes, Special Publication 17* (eds. P. M. Huang and M. Schnitzer). Soil Science Society of America, Inc., Madison, WI, pp. 1–27.

Torn M. S., Trumbore S. E., Chadwick O. A., Vitousek P. M. and Hendricks D. M. (1997) Mineral control of soil organic carbon storage and turnover. *Nature* **389**, 170–173.

Veldkamp E. (1994) Organic carbon turnover in three tropical soils under pasture after deforestation. *Soil Sci. Soc. Am. J.* **58**, 175–180.

von Lützow M., Kogel-Knabner I., Ekschmitt K., Matzner E., Guggenberger G., Marschner B. and Flessa H. (2006) Stabilization of organic matter in temperature soils: mechanisms and their relevance under different soil conditions – a review. *Eur. J. Soil Sci.* **57**, 426–445.

Wagai R. and Sollins P. (2002) Biodegradation and regeneration of water-soluble carbon in a forest soil: leaching column study. *Biol. Fert. Soils* **35**, 18–26.

Zech W. and Guggenberger G. (1996) Organic matter dynamics in forest soils of temperate and tropical ecosystems. In *Humic Substances in Terrestrial Ecosystems* (ed. A. Piccolo). Elsevier, Amsterdam, pp. 101–170.

Zhou Q., Maurice P. A. and Cabaniss S. E. (2001) Size fractionation upon adsorption of fulvic acid on goethite: Equilibrium and kinetic studies. *Geochim. Cosmochim. Acta* **65**, 803–812.

Zibilske L. M. (1994) Carbon mineralization. In *Methods of Soil Analysis Part 2: Microbiological and Biochemical Properties* (eds. R. W. Weaver, S. Angle and P. Bottomley). Soil Science Society of America, Inc., Madison, WI, pp. 835–864.

Zsolnay A. (1996) Dissolved humus in soil waters. In *Humic Substances in Terrestrial Ecosystems* (ed. A. Piccolo). Elsevier, Amsterdam, pp. 225–264.

Zunino H. and Martin J. P. (1977) Metal-binding organic macromolecules in soil: 1. Hypothesis interpreting the role of soil organic matter in the translocation of metal ions from rocks to biological systems. *Soil Sci.* **123**, 65–76.

Associate editor: Jack J. Middelburg